Multiscaling properties of rain in the time domain, taking into account rain support biases

Sébastien Verrier, Cécile Mallet, Laurent Barthès

Multiscaling properties of rain in the time domain, taking into account rain support biases

S. Verrier,[1] C. Mallet,[1] and L. Barthès[1]

Received 26 January 2011; revised 25 July 2011; accepted 25 July 2011; published 26 October 2011.

[1] A number of studies have shown that rainfall processes may be described by stochastic scaling models in the time domain. However, most of the data sets have a resolution that is too limited to perceive the internal structure and variability of rain events. In this study, we analyze high-resolution (15 s) disdrometer time series, of total duration 2 years, obtained in Palaiseau, France. Monofractal and multifractal analysis tools are applied to the data set in order to investigate the scaling properties of the process, especially within the framework of universal multifractals (UMs). From spectral analysis and first-order structure function, it is shown that rainfall should be modeled by nonconservative (integrated) processes at small scales (hourly or finer) but not at larger scales. Multifractal analysis shows that two multiscaling regimes should be distinguished, i.e., ~3 days to 30 min and 15 min to 15 s, with different UM parameters. The former is likely to represent the interevent variability, and the latter is likely to represent the event internal variability. Moreover, most data points contain zero values, which are susceptible to bias multifractal analysis results. In order to assess the effect of the zeros on multifractal analysis results, the UM parameters are also estimated from two variants: from uninterrupted rain events (with almost no zeros) and from a modified (weighted) version of analysis procedure that overweights nonzero values. The parameters are shown to depend noticeably on the proportion of zeros. We propose an approach based on a scaling support of the time series and derive semitheoretical formulas for the bias in the parameters, which are applied in our case study. Finally, we discuss the advantages and drawbacks of some models for numerical simulation of multifractal fields containing a lot of zeros.

Citation: Verrier, S., C. Mallet, and L. Barthès (2011), Multiscaling properties of rain in the time domain, taking into account rain support biases, *J. Geophys. Res.*, *116*, D20119, doi:10.1029/2011JD015719.

1. Introduction

[2] Rainfall displays a very heterogeneous behavior, in a twofold way. First, wet and dry periods alternate and may have variable duration. On the other hand, there is also an extreme variability in the interior of rain events. Since rainfall dynamics involve a wide range of time scales and space scales, scaling models have been considered for a long time by researchers. These models display features such as power law spectra, induced by the absence of characteristic scale in a given range of scales (usually coined as scaling range). Such power laws are accurately displayed by rainfall data sets, at least for some scaling ranges. Scaling behaviors seem even to occur in most geophysical fields. However, it has appeared to geophysicists that usual simple scaling (monofractal) models, characterized by a single fractal dimension, may represent an artificially narrow class of processes, with a too-limited variability. In other words, power spectra are useful when determining the existence of one or several scaling regime(s), but since it is a second-order statistic, some information about low-order or high-order statistics is missed. The latter point is especially crucial when considering the most rare and extreme events, the most important ones for operational hydrology, civil engineering, and safety policies. Then, more elaborated models have been designed, in order to account for a wide set of (decreasing) fractal dimensions, associated with increasingly high intensities. These are multifractal models, characterized by an infinite spectrum of fractal dimensions. A popular route to multifractality is that of stochastic multiplicative cascades, first developed in the context of statistical modeling of turbulence [*Kolmogorov*, 1962; *Obukhov*, 1962; *Yaglom*, 1966; *Mandelbrot*, 1974]. In a general manner, cascade models rely on three phenomenological assumptions: (1) there exists a quantity (energy flux in the context of turbulence) which is conserved *in average* from large to smaller scales; (2) this quantity is heterogeneously transmitted to smaller scales in a scale-invariant way; and (3) most of the interactions occur between neighboring scales. Moreover, the cascade is said

[1]LATMOS, CNRS/INSU, Université de Versailles Saint-Quentin-en-Yvelines, Guyancourt, France.

0148-0227/11/2011JD015719

multiplicative when its heterogeneity is built by an iterative multiplicative modulation process. This results in a multifractality that would need, in principle, an infinite number of parameters (i.e., an infinite set of fractal dimensions). Yet, it has been shown that under plausible assumptions, (continuous in scale) cascades converge toward laws that are often characterized by a small number of degrees of freedom (universality). For instance, the universal multifractal (UM) model [*Schertzer and Lovejoy*, 1987] (that includes the well-known special case of lognormal cascades, with $\alpha = 2$) and the log-Poisson model [*She and Levêque*, 1994] need only two fundamental parameters. For 25 years, scientists have performed multifractal analysis over a number of geophysical fields, leading to the conclusion that multifractality should be somewhat ubiquitous in nonlinear geophysics (for reviews, see *Lovejoy and Schertzer* [2007, 2010]). In particular, the multifractality of rain, first proposed by *Schertzer and Lovejoy* [1987], has been confirmed by a number of studies in the time and space domains (for reviews, see *Lovejoy and Schertzer* [1995], *Lilley et al.* [2006], and even in a spatio-temporal framework *Marsan et al.* [1996], *Over and Gupta* [1996], and *Deidda* [2000]). The multifractal structure of rainfall time series has been investigated by a number of papers, e.g., in the UM framework [*Ladoy et al.*, 1991; *Tessier et al.*, 1993; *Hubert et al.*, 1993; *Ladoy et al.*, 1993; *Olsson*, 1995; *Harris et al.*, 1996; *Schmitt et al.*, 1998; *de Lima and Grasman*, 1999; *Pathirana et al.*, 2003; *de Lima and de Lima*, 2009; *Sun and Barros*, 2010; *Lovejoy et al.*, 2011]. The main results (scaling regimes, UM parameters) of these papers are recalled in Table 1. As shown, most of the studies suffer from the limited resolution of the data (typically one day). Obviously, rain has much variability at subdaily scales, hence some singular behavior should be expected at these small time scales. Recently, *de Montera et al.* [2009] have performed multifractal analysis of high-resolution (<1 min) time series obtained by the means of a dual-beam spectropluviometer. They found the existence of a break in the scaling at 1 hr time scale, and of a scaling regime, in the interior of rain events, with UM parameters far from the usual large-scale ones (see Table 1). They advocated that the break at 1 hr time scale could be due to the presence of numerous zeros in the series, which would lead to biases in multifractal analysis at larger scales. It is perhaps not well known enough that the presence of these zeros may considerably affect the estimation of multifractal parameters, even though this has been noticed for a long time [*Harris et al.*, 1996; *Schmitt et al.*, 1998]; see also *Fraedrich and Larnder* [1993] in a monoscaling framework. Such a phenomenon may be easily retrieved by analyzing thresholded synthetic multifractal fields [*Verrier et al.*, 2010]. Other comments on the effects of thresholds on rain spatial statistics may be found in the work of *Lovejoy et al.* [2008]. In the time domain, the transition at ~1 h may be viewed as a transition from a multiscaling regime to another with different parameters (including a transition from nonconservativity to conservativity). However, the physical interpretation of the transition remains unclear but could involve a kind of threshold in the rain generation process.

[3] The present paper aims to extend the results obtained by *de Montera et al.* [2009], using another high-resolution time series covering a wide range of scales (2 years of rain intensity data at 15 s resolution). The present study will distinguish the main scaling regimes of rainfall in the time domain in the range of scales available from the measurements. Different analysis procedures will be performed in order to highlight the role of the zero rain rates. Furthermore, a semitheoretical explanation and formulas for the biases observed in UM parameters estimates on data sets that contain a lot of zeros will be proposed and tested.

[4] The study is structured as follows. In section 2, the main properties of the multifractal formalism are recalled, including UM parametrization. Section 3 provides information on the data set and the experiment. As a first step, some monoscaling analysis techniques were applied to the series in order to determine the scaling regimes; the results are presented in section 4. Then, section 5 exposes the application of classical multifractal analysis tools to the series and to rain events extracted from the series. The latter procedure aims to distinguish between rain variability in rain events and the alternation between rain and absence of rain and to characterize the scaling properties of the former. UM parameters are shown to be strongly different at large scale, compared to those estimated from (small-scale) rain events. It is suggested that at least part of the difference may be due to the zero rain rates. In section 6, some suggestions for modeling multifractal fields that have many zeros are proposed. From a model of scaling support, semitheoretical formulas are derived to quantify the bias of multifractal analysis results depending on the codimension of the support. We also review and discuss the advantages and drawbacks of existing models of support generation. It is argued that a thresholded multifractal model could be able to reproduce some of the observed features of the DBS series. Finally, we conclude in section 7.

2. Some Theories of Multifractals

2.1. Multiplicative Cascades and Multifractals

[5] Multiplicative cascades are defined by an iterative multiplicative construction as follows. First, distribute uniformly a quantity at the largest scale T of the process (called external scale), i.e., over a full interval $[0, T]$. Then, divide the initial interval in λ_1 (usually, two) subintervals of equal length (or, in D dimensions, in λ_1^D subpixels or subhypercubes). Attribute a value on each subinterval by multiplying the initial value by a random variable. Then, repeat the construction by subdividing each of the previous subintervals in λ_1 new subintervals and attribute a value to each of the new intervals. By iterating the process, you can build a series $\Phi_\lambda(t)$ of resolution $\lambda = \lambda_1^n$ (in the following, the resolution varies as the inverse of the interval length, which is the time scale, $\lambda = T/\Delta t$). If we impose all random variables to be independent and identically distributed and distributed independently of the scale, one can obtain a series (or a field) that has scale-invariant properties. Usually, the mean of the process is assumed to be statistically conserved when the resolution changes: $\forall \lambda, \langle \Phi_\lambda \rangle = M$.

[6] The latter equation expresses canonical conservation, which will be considered in the scope of this paper. Note that conservation can also be defined in a microcanonical way (see *Mandelbrot* [1974] about this distinction), i.e., exact conservation at each step.

[7] Generically, scale-invariant multiplicative cascades converge toward multifractal fields [see, e.g., *Schertzer*

Table 1. Comparison of Universal Parameters α, C_1, H, and Empirical Spectral Slope β, Estimated Over Various Ranges of Time Scales[a]

Reference	Measurement	Range of Scales	α	C_1	H	β
Tessier et al. [1993]	Gauges, daily accumulations	1–64 days	0.55	0.6	-	-
Ladoy et al. [1993]	One gauge, daily accumulations	1–64 days	0.45	0.60	0.03[a]	0.37
Fraedrich and Larnder [1993]	Rain gauges (daily and 5 min resolutions)	3 days to 2.4 h	-	-	-	0.5
		<2.4 h	-	-	-	1
Olsson [1995]	Gauges, 2 years of 8 min data	(3–11) days to 8 min	0.63	0.44	0.10[a]	0.66
Tessier et al. [1996]	Gauges, daily accumulations	15 days to 1 day	0.7	0.4	−0.1	0.4
de Lima and Grasman [1999]	Nonrecording gauge (daily resolution)	8–128 days	0.66	0.30	−0.23[a]	0.17
		1–8 days	0.48	0.51	−0.11[a]	0.17
	Recording gauge (15 min resolution)	15 min to 10.7 days	0.49	0.51	−0.02	-
Pathirana et al. [2003]	Gauges, hourly accumulations	1 day to 1 h	1.35	0.34	−0.05	1.02
Molini et al. [2009]	Rain gauges, accumulations (up to 60 min)	3 days to 2 h	-	-	-	0.7
de Lima and de Lima [2009]	Gauges, daily records	1–16 days	0.5–0.7	0.35–0.5	−0.13	-
de Montera et al. [2009]	Dual-beam spectropluviometer	>1 h	0.24	0.63	0	-
	Dual-beam spectropluviometer, uninterrupted rain events	1 h to 1 min (full rain)	1.69	0.13	0.53	-
Lovejoy et al. [2011]	Gauges (hourly data gridded on 2.5° × 2° pixels)	>3 months	-	-	-0.42	0.08
		(2–10) days to 1 h	-	0.37	0.17	0.76

[a]These values of H were not explicitly estimated by the cited authors yet may be deduced from the exponents α, C_1, and β they found and from the relationship $\beta = 1 - K(2) + 2H$.

et al., 2002]. The fundamental equation of the (codimension) multifractal formalism expresses the fact that for a multifractal field, the probability of exceedence of a threshold that is power law of the resolution is also power law with exponent depending on the amplitude of the family of thresholds:

$$\Pr(\Phi_\lambda > \lambda^\gamma) \approx \lambda^{-c(\gamma)} \tag{1}$$

where Φ_λ is the (normalized, $M = 1$) series or field seen at resolution λ and $\approx$ indicates an equality within the limits of slowly varying functions. Above, the (real) exponent γ is a scale-invariant indicator of the amplitude of the resolution-dependent family of thresholds:

$$T_\lambda = \lambda^\gamma \tag{2}$$

Here, γ is called singularity and characterizes the amplitude of the process independently of the scale. It is associated to a unique fractal codimension denoted $c(\gamma)$, which is the exponent of the power law defined in (1). By varying the singularity, we can describe the fractal codimensions of families of thresholds of various amplitudes. Physically, the higher the threshold, the more intense the events: it is expected that higher singularities are associated with the most rare events, with smaller fractal dimensions: $c(\gamma)$ increases with γ. $c(\gamma)$ defines a function, called codimension function, which entirely characterizes the multifractal series or field Φ_λ. Note that the trivial case $c(\gamma) = const$ corresponds to monofractality. In a general manner, $c(\gamma)$ is convex, positive, with a fixed point C_1 imposed by the condition of canonical conservation. Since the probability distributions are closely related with the statistical moments, (1) is equivalent [*Schertzer and Lovejoy*, 1987] to:

$$\langle \Phi_\lambda^q \rangle \approx \lambda^{K(q)} \tag{3}$$

where $\langle \bullet \rangle$ denotes the averaging operator, q is the (non-necessarily integer) order of the moment, and $K(q)$ is the moment scaling function. Equation (3) expresses that the moments of the series, at fixed order, depend in a power law way of the resolution. The high orders obviously correspond to the highest values of the series and also to the highest singularities. In fact, the analogy is closer since there is a one-to-one correspondence between singularities and moment orders, since the moment scaling function is the Legendre transform of the codimension function [*Parisi and Frisch*, 1985]. In the same way, it may be demonstrated that $K(q)$ should be convex. Because of the imposed scale-by-scale conservation of the mean, we have $K(1) = 0$. For a space-filling field, we also have $K(0) = 0$ (more generally, $-K(0)$ is the codimension of the support; see section 6.

[8] The characterization of a multifractal field needs the knowledge of the moment scaling function, or equivalently of the codimension function, which describe the statistics at all scales.

2.2. Universality

[9] Because of the small number of constraints that apply a priori on $K(q)$, i.e., convexity and trivial values, a great variety of possible functions could be involved. The characterization of the multifractal properties would therefore need an infinite number of parameters, which is unmanageable. Various attempts to reduce the number of parameters to a limited number of physically relevant ones have been proposed. In addition, such models should have some attractor properties in order to be physically realistic. Such properties may appear, under certain conditions, with continuous in-scale cascades. Obviously, the classical discrete cascades (where λ is necessarily an entire power of an elementary step λ_1) are not physically realistic since (1) the step λ_1 has no physical justification and (2) they induce an artificial clustering of the data in square-like shapes. On the contrary, physically relevant cascades should be continuous in scale, i.e., with $\lambda_1 \to 1$, which is equivalent to add more and more (up to infinity) steps between the initially discrete steps. Since continuous in-scale multiplicative cascades converge by construction to log-infinitely divisible distributions, the possible choice of random generators has been restricted, and at least some of them need few degrees of freedom. Some authors have proposed log-Poisson statistics [*She and Levêque*, 1994; *Dubrulle*, 1994; *She and Waymire*, 1995]. On the contrary, by assuming stability of the generator and suitable renormalization, *Schertzer and Lovejoy* [1987, 1991] have proposed log-Levy statistics,

defining the UM model. Mathematical and physical arguments supporting this kind of (strong) universality, may be found in the work of *Schertzer and Lovejoy* [1997]; see, however, *Gupta and Waymire* [1997] for discussion about the generality of this model. Yet, this model has been applied successfully to a number of geophysical fields [*Lovejoy and Schertzer*, 2010]. UM fields have the following parametrized moment scaling function:

$$K(q) = \frac{C_1}{\alpha - 1}(q^\alpha - q). \quad (4)$$

[10] There are two relevant parameters: α, the index of multifractality, which is between 0 (monofractality) and 2 (lognormality); and C_1, which is the codimension giving the dominant contribution to the mean value of the field. The higher the C_1, the more intermittent the field: then, peaks become more sparse but higher. C_1 is bounded below by 0 (homogeneity) and above by the dimension of the embedding space, denoted D. Because of Legendre transform, $C_1 = c(C_1) = K'(1)$ is the fixed point of the codimension function as well as the singularity associated with the mean (moment of order 1).

2.3. The FIF Model

[11] Since most geophysical fields are nonconservative, an extension of the UM model to nonconservative fields has been proposed [*Schertzer and Lovejoy*, 1991]. This is the fractionally integrated flux (FIF) model, based on the fractional integration of a conservative UM. The order of integration, denoted H, defines a nonconservativity parameter: it strongly constrains the smoothness of the field. The FIF model has therefore three parameters. A FIF series has stationary increments, following:

$$|R_\lambda(t + \Delta t) - R_\lambda(t)| \stackrel{d}{=} \Phi_\lambda |\Delta t|^H \quad (5)$$

where $|\Delta t| = \frac{T}{\lambda}$.

[12] The FIF model is especially useful to model scaling processes with spectral exponent greater than 1. Indeed, the power spectrum of a multifractal FIF follows a power law $E(k) \propto k^{-\beta}$ where k is the wave number and $\beta = 1 - K(2) + 2H$ is the spectral exponent. Of course, the formula holds in the case of conservative cascades, with $H = 0$. Note that the power spectrum is a second-order statistic, hence the term $K(2)$. The determination of the parameter H may be done with the help of first-order structure function, namely, $\langle |R_\lambda(t + \Delta t) - R_\lambda(t)| \rangle = f(\Delta t) \propto |\Delta t|^H$.

3. The Data Set

[13] A dual-beam spectropluviometer (DBS) has performed more than 2 years of measurements in Palaiseau, near Paris, France. This instrument uses two flat parallel infrared beams of 2 mm in height, 40 mm in width and 250 mm in length, hence has a 100 cm^2 catchment surface. The two beams help detection of small drops to be performed, down to 0.3 mm in diameter. Various means of reducing instrumental and physical disturbances and false detections have been used, that are presented by *Delahaye et al.* [2006]. The device provided diameters, fall velocities and times of arrival of raindrops. From the latter, the rain rates are estimated at 1 s resolution. Since rain typically decouples from turbulence at scales smaller than 1 m [*Lovejoy and Schertzer*, 2008], it should be expected that a scaling behavior could hold up to 1 s time scale. However, measurement limitations seem to be dominant at such small scales with this instrument, and that a larger integration time should be necessary. In this study, the rain rates were estimated over an integration time of 15 s. The validity of the latter will be justified a posteriori in section 4. In order to facilitate multifractal analysis, a 2^n section has been extracted from the raw data set, covering approximately 96% of the latter. Therefore, the data set consists of a 15 s rain rate time series of length 2^{22} points and spans almost a 2 year period. After correction of some unreliable small portions of the series, a threshold of 0.1 mm h has been applied in order to wash out doubtfully low values. The main properties of the data set are summarized in Table 2. An example of rain event, measured by the DBS on 12 May 2009, is shown in Figure 1. However, similar rain events represent only a small part of the total series. From Table 2, it may be noticed that most points of the series contain a (true or instrumental) zero rain rate value. The latter may impact rainfall stochastic modeling, which will be discussed in sections 5 and 6.

4. Some Evidence of Scaling

[14] This section investigates the scaling properties of the series and of its support, independently of a particular (multi) fractal model. The purpose is to determine the scaling regimes of the series from classical tools such as power spectrum and (slightly modified) box-counting algorithm.

4.1. Power Spectrum

[15] Consistently with the remarks of section 2.3, a scaling regime is generically associated with a power law portion of spectrum. The power spectrum of the DBS series, averaged over logarithmically spaced bins, is provided in Figure 2 (in log-log coordinates). At time scales greater than a few days, the spectrum is almost flat. This is coherent with the findings of most papers [see, e.g., *Ladoy et al.*, 1993; *Fraedrich and Larnder*, 1993; *Tessier et al.*, 1996; *Lovejoy et al.*, 2011. However, the very low value of the spectral slope (the so-called "spectral plateau") at scales greater than a few days or weeks should not be misinterpreted or overinterpreted since this single information is not sufficient to reject the hypothesis of long-range dependencies [*Lovejoy et al.*, 2011].

[16] At the higher frequencies, a scaling regime appears clearly at time scales between 30 s and 30 min time scales. In this range of scales, the spectral slope is $\beta = 1.55 \pm 0.03$ (the error bar corresponds to the 95% confidence interval). The latter value is greater than 1, which means that, in case of multifractality, a nonconservative model (such as the FIF model) should be more appropriate (see also section 4.3). There is almost no flattening at the far highest wave numbers, meaning that measurement would be affected by a very moderate level of measurement noise at the series resolution, which remains coherent with the findings of *de Montera et al.* [2009], based on the same instrument, but from measurements obtained in different periods and places. This justifies a posteriori the choice of the resolution of the

Table 2. Properties of the Preprocessed DBS Time Series Used in This Study

Property	Value
Date and Time (Beginning)	16 July 2008 15:00:00
Date and time (end)	14 July 2010 16:15:45
Resolution	15 s
Series length	2^{22}
Mean	0.052 mm h
Percentage of zeros	95.9%
Threshold	0.1 mm h

series explained in section 3. The time scales between 3 days and 30 min correspond to a slow transition from the large-scale flat spectrum to the small-scale scaling regime. Two indicative fits within this range of scales are shown in Figure 2, illustrating that the spectral slope is smaller at smaller frequencies (with slopes $\beta = 0.41 \pm 0.06$ and 1.09 ± 0.07 for 3 days to 3 h and 3 h to 30 min ranges, respectively). The properties deduced from Figure 2 seem rather coherent with some results of literature that are based on high-resolution data. As reported in Table 1, a scaling break at 1–5 days has been found by *Fraedrich and Larnder* [1993], *Olsson* [1995], *Pathirana et al.* [2003], *Molini et al.* [2009], and *Lovejoy et al.* [2011]. The spectral slopes they estimated, for subdaily scales, were between 0.5 and 1. They did not, however, notice any higher spectral slope at subhourly scales, probably because their work was based on data at coarser resolutions than ours. Opposite, *de Montera et al.* [2009] have found a specific scaling regime at subhourly scales, with a spectral slope greater than 1, and with a nonconservativity exponent $H \sim 0.5$. These results suggest the existence of a nonconservative scaling regime at the subhourly scales, coherently with our findings, i.e., with the 30 min to 30 s scaling regime highlighted above. Similarly with the results of *de Montera et al.* [2009], this scaling behavior holds well up to subminute scales and would be probably mainly limited by the measurement noise, at scales of several seconds.

[17] The small-scale estimate of β ($= 1.55 \pm 0.03$) in Figure 2 needs some comments, since it is remindful (with a slight but significant difference) of the classical value 5/3 of the Corrsin-Obukhov law of passive scalars [*Obukhov*, 1949; *Corrsin*, 1951]. Even though rain is not a passive scalar, it is strongly coupled with turbulence. In particular, turbulence strongly accelerates the growth of small cloud droplets and therefore rain initiation, by increasing the mean collision rate [*Falkovich et al.*, 2002; *Xue et al.*, 2008; *Wang and Grabowski*, 2009]. Furthermore, rainfall may share some properties with passive scalars. Of course, individual raindrops are far too heavy to behave like passive scalars, especially they are characterized by too large Stokes numbers. However, it has been recently demonstrated [*Lovejoy and Schertzer*, 2008] that patches of raindrops are likely to display such a behavior above a spatial critical scale l_c. In the latter paper, the authors used three-dimensional raindrop stereophotography data in a 10 m^3 volume and showed that the liquid water density power spectrum accurately follows a $k^{-5/3}$ law above a critical scale l_c of the order of 50 cm. A passive scalarlike model for rain has recently been proposed by *de Montera et al.* [2010] under some plausible physical assumptions. The authors checked the predictions of their model up to storm scale, based on radar and disdrometer data.

[18] In our present case study, several reasons may therefore contribute to the difference between the small-scale value of β in Figure 2 and the "expectable" 5/3 value. Multifractal "intermittency" corrections to the spectral slope could be involved. These corrections are closely related with multifractal parameters, as expressed by the equation $\beta = 1 - K(2) + 2H$ (see section 2.3). In sections 4.3 and 5.2, UM and nonconservativity exponents will be estimated in a similar scaling regime. The parameters will be such that $K(2) = 0.24$ and $H = 0.38$, hence $\beta = 1.52$. Still, a more realistic (passive scalarlike) model of rainfall should involve at least two fluxes, as proposed by *de Montera et al.* [2010]. Moreover, as discussed in sections 5 and 6, the zeros of rainfall may strongly affect scaling properties. Even though this effect will be shown to act mainly at large scales (coherently with Figure 2), it remains possible that the spectral slope could be slightly shifted at smaller scales.

4.2. The Fractality of the Data Set Support

[19] In this section, we focus on the properties of the rain support. The alternation of rain and absence of rain is expected indeed to have some scaling properties, following the results of various studies in the time domain [*Hubert et al.*, 1989; *Olsson et al.*, 1993; *Lavergnat and Golé*, 1998; *Schmitt et al.*, 1998]. In Figure 3, the probability of occurrence of nonzero values is presented as a function of the resolution λ, in logarithmic coordinates. It is shown that, from 1.5 day time scale to 30 min time scale, the probability that a point belongs to the series support follows a power law of the resolution:

$$\Pr(R_\lambda(t) > 0) \propto \lambda^{-c_f} \tag{6}$$

where c_f is a fractal codimension, clearly that of the data set support. In a classical multifractal framework, it would be the codimension associated with the $-\infty$ singularity.

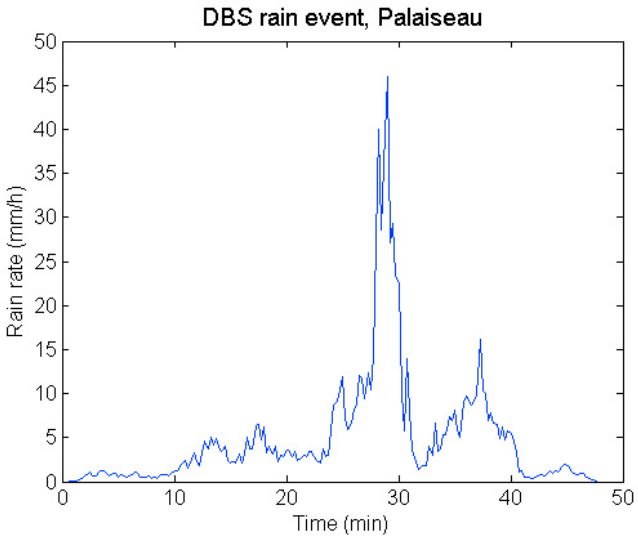

Figure 1. Rain event observed by the DBS on 12 May 2009, beginning at 04:05:00, in Palaiseau.

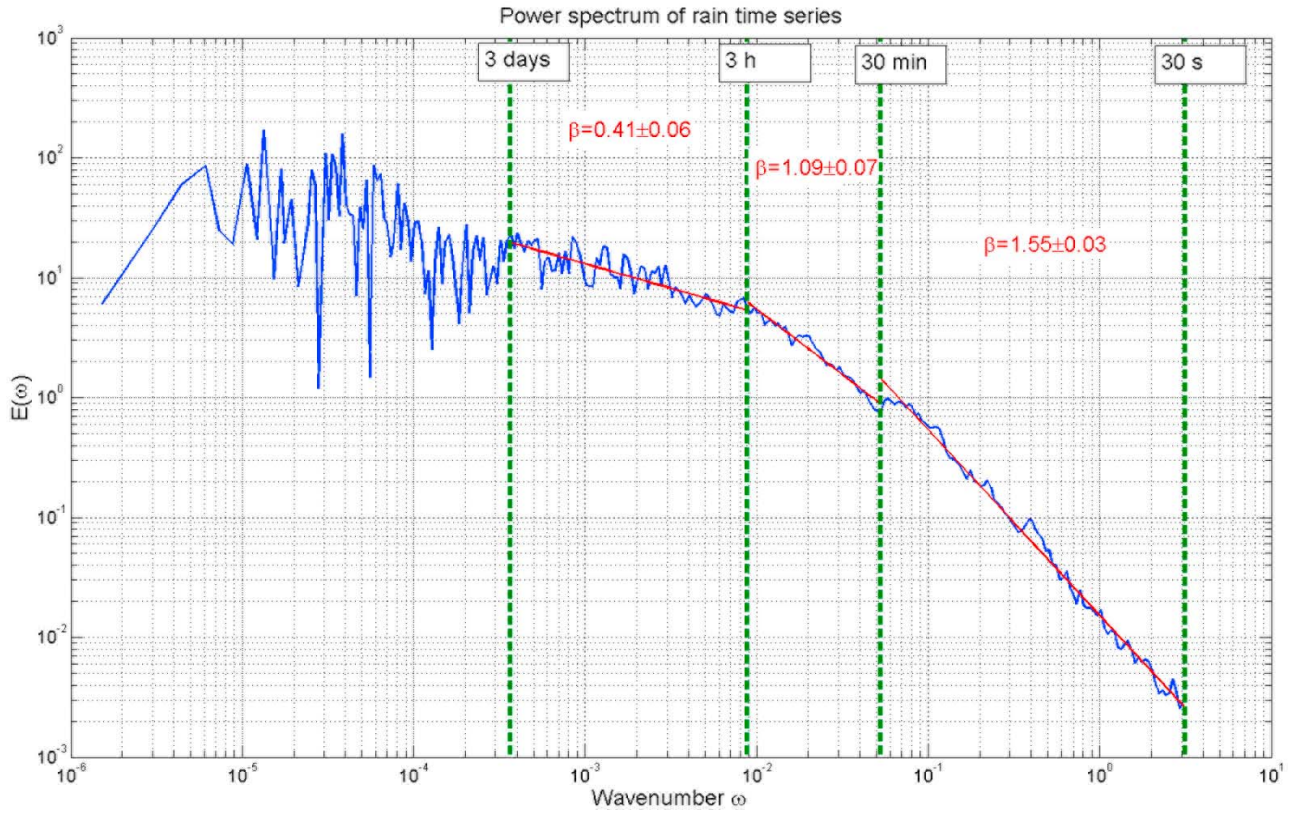

Figure 2. Power spectrum of the DBS rain rate time series and corresponding scaling regimes. Coordinates are logarithmic and wave numbers are normalized, such that the Nyquist wave number is associated with the value π.

[20] It should be pointed out that c_f is representative of the data set support scaling and not of the "true" rain support possible scaling. Indeed, any measurement involves a kind of measurement threshold thus true zero rain rates cannot easily be distinguished from instrumentally defined ones. This may directly impact the observed value of the fractal dimension. Nevertheless, the scaling regimes are expected to hold approximately for comparable thresholds and the estimated data set codimension c_f should be an upper bound of the "true" rain support codimension. In order to eliminate possibly unreliable low rain rates estimation, a threshold of 0.1 mm h has been applied in the DBS series preprocessing. The latter threshold could seem a bit high, however, its choice was motivated by the necessity to remove instrumental noise and false detections. From the fit in Figure 3, the data set codimension is estimated at 0.45, meaning that in the corresponding scaling range, the data set is embedded in a fractal support of dimension $d_f = 0.55$. To illustrate the dependence of the fractal dimensions on the threshold, it should be emphasized that a threshold of 0.01 mm h in DBS preprocessing would have shifted the codimension value to 0.40. This dependence is rather strong since support codimensions are equivalent to 0-order statistics. However, the reference DBS data set, thresholded at 0.1 mm h, will be considered in sections 4 and 5, where higher-order statistics are of interest.

[21] As stated previously, the codimension of the data set support is estimated at 0.45, meaning that in the corresponding scaling range (1.5 days to 30 min), the data set is embedded in a fractal support of dimension 0.55. Because of the dependence of fractal dimensions on thresholds, direct comparison with other literature results is nontrivial. However, *Schmitt et al.* [1998] found a scaling regime for their data set support that extends from 3 day to 10 min time scales. They also found a support dimension of 0.55, which is difficult to compare with our estimate because of a different measurement resolution and threshold. We should also mention the study by *Olsson et al.* [1993] who distinguish three scaling regimes separated by transitions at 1 week and 45 min time scales. In the 1 week to 45 min regime, these authors estimated a fractal dimension of 0.37. Moreover, they found a pseudoscaling regime of dimension 1 in the range 2 years to 1 week, which is rather coherent with Figure 3 where the probability of nonzero rain values becomes almost constant after a few days, i.e., $c_f = 0$. Such a behavior is in fact not surprising: at large scales, large time intervals ($\gg$1 day) almost surely contain a rain event. From Figure 3, the support does not seem scaling at scales smaller than 30 min, except perhaps at the far smallest scales. The probability of occurrence of rain is greater than predicted by prolonging the power law that holds between 1.5 days and 30 min. This may be due to the fact that this range of scales is dominated by continuous rain events that do not contain zeros. However, if a scaling behavior still holds (which is not obvious in Figure 3), the support is expected to have a greater dimension. *Olsson et al.* [1993] have tried to estimate fractal dimensions in the range 1–45 min, and found 0.82.

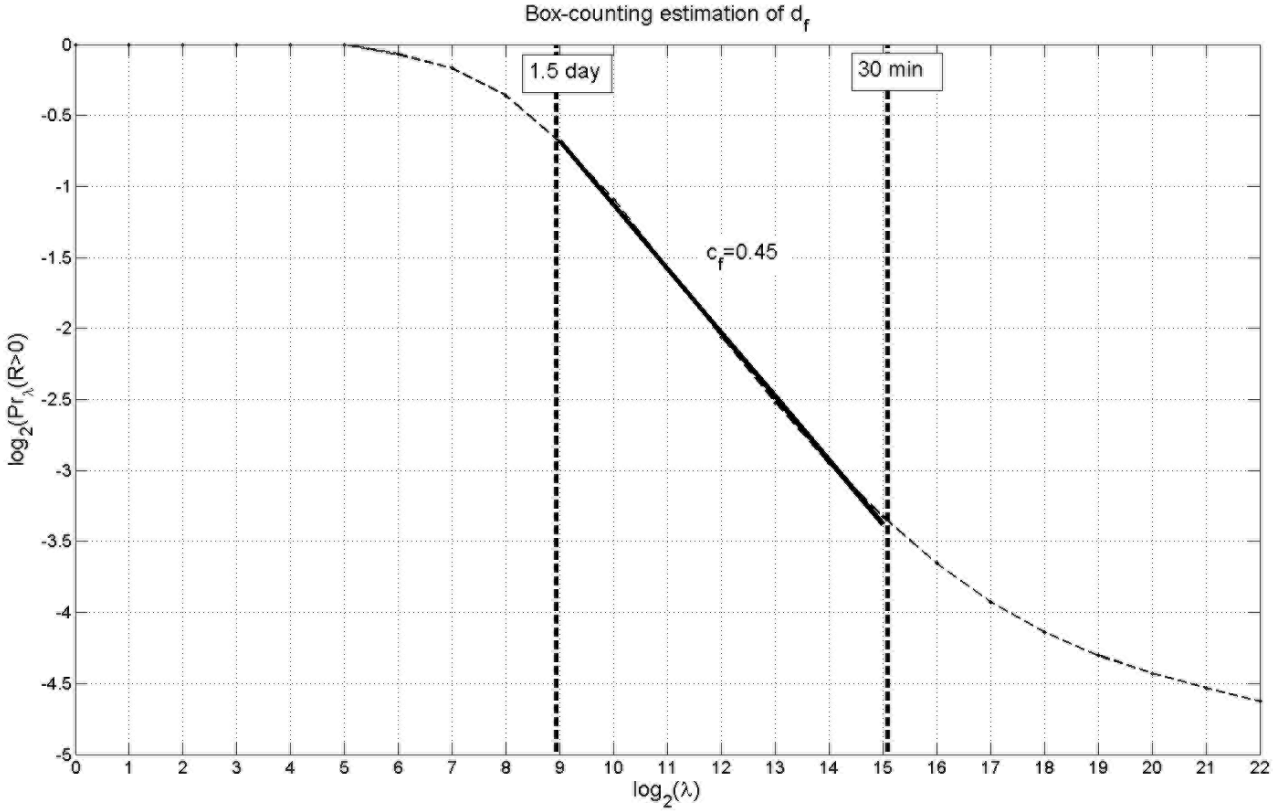

Figure 3. Probabilities of nonzero series values as a function of the resolution. The fractal codimension of series support is deduced. This algorithm could be viewed as a probabilistic variant of the classical box-counting algorithm.

4.3. Structure Function Analysis

[22] As stated in section 2.3, the nonconservativity exponent H may be estimated directly from the first-order structure function of the series. From spectral slopes, it may be conjectured that the rain process will have a nonconservativity exponent $H \leq 0$ at large scales, but $H > 0$ at scales smaller than 3 h (where $\beta > 1$). The first-order structure function of the series, $f(\Delta t) = \langle |\Delta R(\Delta t)| \rangle$ is represented in logarithmic coordinates in Figure 4, as a function of time increment. The structure function is completely flat at scales greater than 6 h, meaning that at these scales conservative (or fractionally differentiated) multifractal fluxes should be involved, without any additional integration. In the range of scales 3 days to 3 h, this result has to be compared with the values that can be deduced from the relation $\beta = 1 - K(2) + 2H$ with $\beta = 0.41$ and (as discussed further in section 5.2, see also Table 3) $K(2) = 0.65$, hence $H = 0.03$: within this range of scales, strict conservation seems tenable, coherently with values reported in Table 1. Nevertheless, strict conservation is unlikely to hold at larger scales (i.e., >1 week) since β and K(2) diminish at very large scales (see also Figure 6) so that $H < 0$. The study of processes that have a strictly negative H exponent is a bit more involved since in this case "incremental" structure functions such as defined above cannot provide a reliable estimation of H and more sophisticated tools would be needed. Recent works [e.g., *Lovejoy et al.*, 2011] investigated in detail the low-frequency scaling of rainfall based on gauge data spanning a few decades and the authors find a large-scale estimate of H close to −0.4.

[23] Considering now the smaller scales, it may be seen that at time scales between 8 min and 6 h, the curve in Figure 4 is nonlinear with a low instantaneous slope. However, at very small time scales (<8 min), the structure function is a power law with exponent $H = 0.38$. This value is not easily comparable with literature results which generally do not investigate such scales. As reported in Table 1, the main exception would be the study of *de Montera et al.* [2009] based on short rain events. One should note that the estimation of H on a data set that contains many zeros may be unreliable. In the space domain, *Verrier et al.* [2010] found that H could be underestimated from such data sets.

[24] The transition from $H > 0$ to $H \sim 0$ at scales of a few hours seems physically relevant in terms of correlation. Indeed, at the smaller scales, the structure of almost uninterrupted rain events presents a high degree of correlation, possibly modeled by an integrated process. Opposite, the properties of coarse scale (i.e., greater than the mean event duration) rain are in fact conditioned by rain events total accumulations, that are less intercorrelated, thus there is no need of an integrated model.

5. The Multiscaling Properties of the DBS Series

5.1. Multifractal Analysis: The Principle

[25] In section 5.1, a classical procedure for investigating multifractality on data is recalled. For more details about a

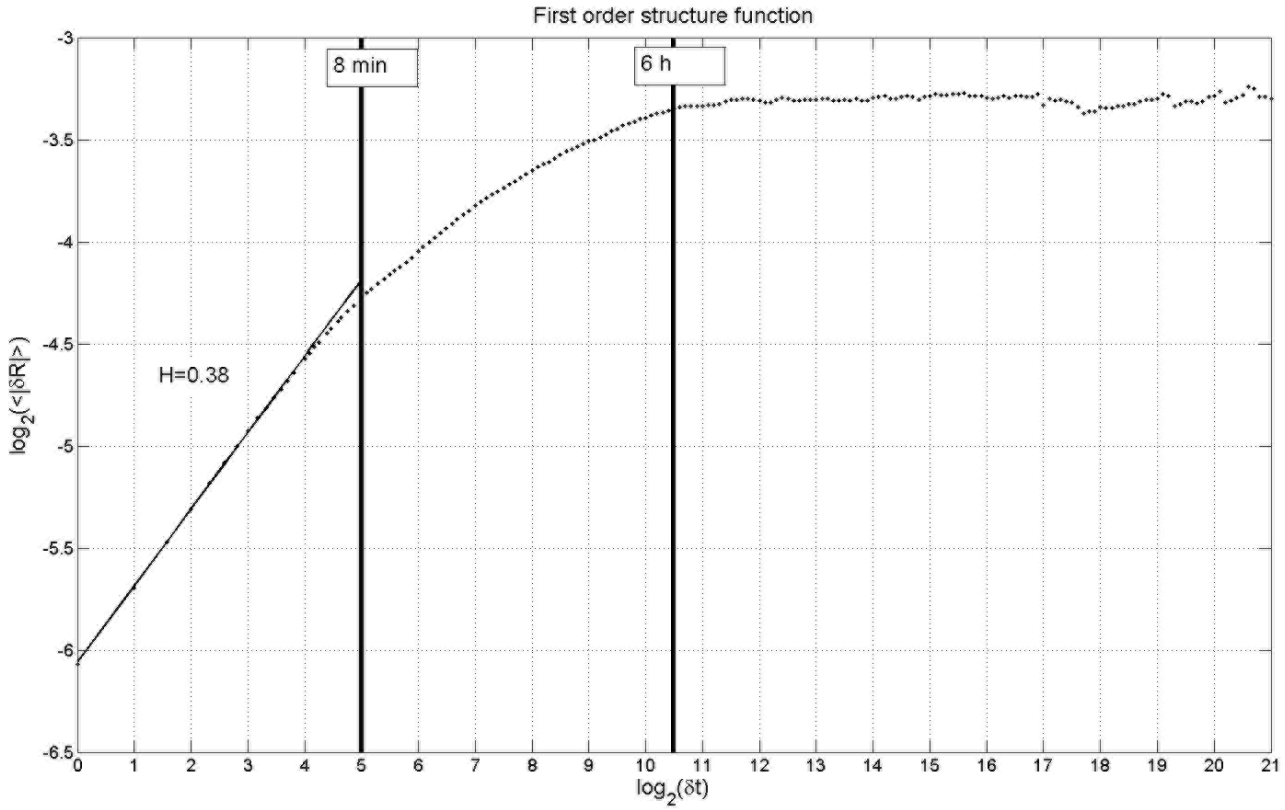

Figure 4. First-order structure function of the DBS time series. Linear regression is used to estimate the small-scale nonconservativity exponent, i.e., $H = 0.38$.

similar methodology, see, e.g., *Tessier et al.* [1993]. The purpose of multifractal analysis (MA) is to test whether the fundamental equation (3) of multifractality is accurately followed. The process may be decomposed in three steps: (1) estimation of the relevant conservative quantity Φ_Λ from the data, at the observation resolution, denoted Λ, (2) degradation of the latter at coarser resolutions, Φ_λ, for $\lambda < \Lambda$, and (3) empirical estimation of the moments for all available resolutions and for various orders q. Step 1 aims to wash out any possible nonconservativity in the data, since the latter may be related to a conservative cascade by a fractional integration. If necessary, a fractional derivative of order H should be necessary to invert the latter. However, it has been shown by *Lavallée et al.* [1993] that, in practice, it suffices to take the normalized absolute gradient at the highest resolution, which is much simpler (and almost as efficient) than a rigorous fractional derivation. In all cases, Φ is normalized by its mean. In step 2, the scale is roughened by iterative steps of factor 2: the values of coarse pixels are deduced from those at double scale by a simple average of neighboring pixels. This procedure therefore approximates the inversion of the multiplicative cascade, even though the latter is supposed to be only statistically conservative. From the estimation of Φ at various resolutions, it is easy to compute the empirical moments for a given interval of orders. Since most literature results report that the statistical moments should diverge at orders greater than a critical order $q_D \approx 3$ [e.g., *Hubert et al.*, 2007], and because of sample size limitations, we restrict the study to an interval of reliable orders which is set to [0, 3]. The moments are then shown on a log-log graph, as a function of the resolution. The presence of straight lines for all orders is therefore the signature of equation (3) and thus of multifractality. A linear fit of the line associated with qth order moment provides the value of $K(q)$: the moment scaling function may therefore be estimated and possibly fitted with

Table 3. Comparison of Universal Parameters α, C_1, H, and Empirical Spectral Slope β Estimated From DBS Data and Different MA Procedures

Data Set + MA Technique	Range of Scales	α	C_1	H	β
DBS whole time series, standard MA	3 days to 32 min	0.31	0.59	0.03[a,b]	0.41[a]
	16 min to 15 s	1.10	0.17	0.38[c]	1.55
DBS 32 min rain events, standard MA	32 min to 15 s	1.84	0.10	0.44	-
DBS whole time series, weighted MA	1 week to 32 min	1.22	0.16	-	-

[a]Spectral and nonconservativity exponents accurate from 32 min to 3–6 h only.
[b]Reporting the large-scale UM parameters and the spectral slope in the formula $\beta = 1 - K(2) + 2H$ leads to $H = 0.03$.
[c]Nonconservativity exponent accurate up to 8 min time scale.

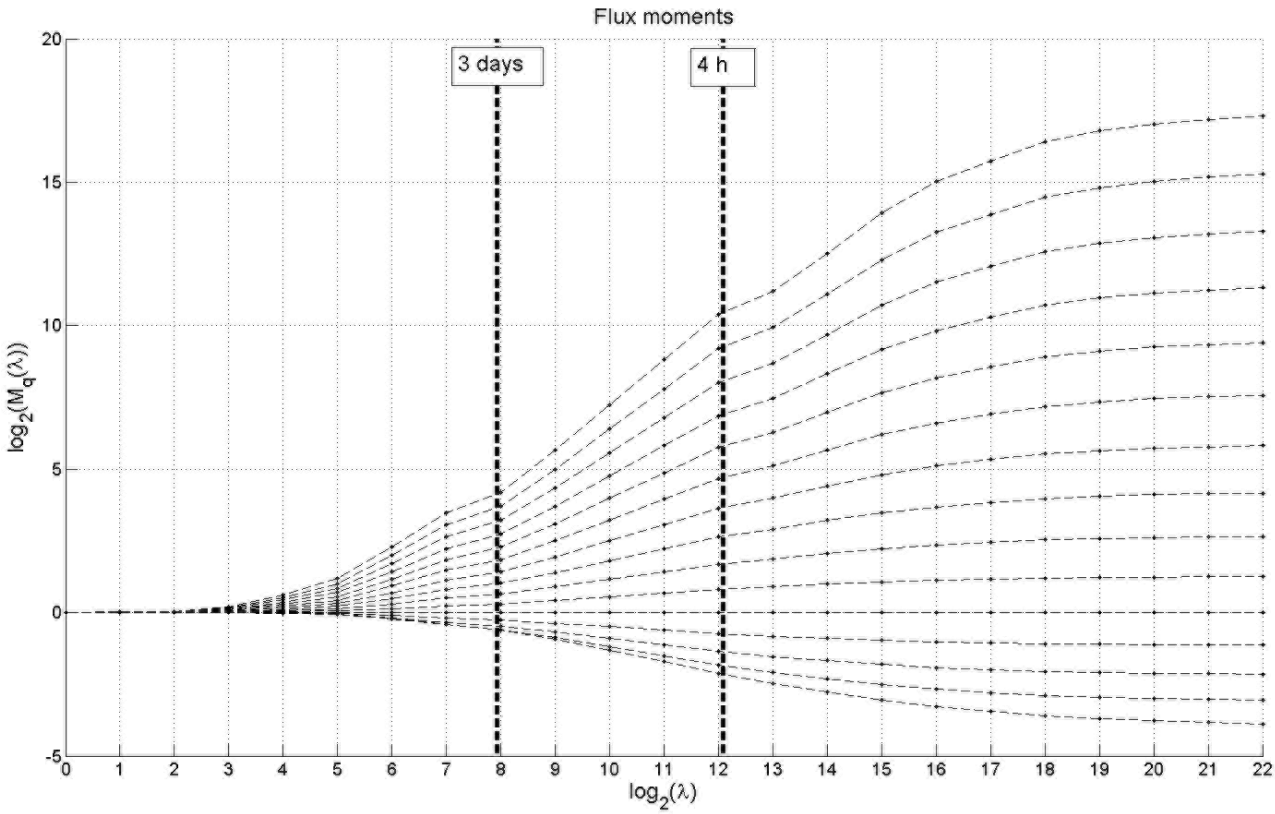

Figure 5. Empirical moments of the DBS time series as functions of the resolution, in log-log coordinates. Each curve corresponds to one specific order of moment, between 0 and 3.

its universal forms. In the latter case, the universal exponents may be estimated.

5.2. Multifractal Analysis of the DBS Series

[26] First, the possible small-scale nonconservativity is not taken into account, i.e., the rain rates are considered directly, without any kind of (finite) differentiation. The graph of the moments of the DBS rain rate series is presented in Figure 5. The logarithm basis is fixed at 2 in order to visualize the successive averagings. A multifractal regime may be found between 3 day and 4 h time scales. On the contrary, a quick view of Figure 5 could lead to think that the process is not multiscaling at scales smaller than half an hour. This would be surprising since the spectrum seems to have good scaling in this domain. However, such a conclusion must not be drawn too quickly, since both spectrum and first-order structure function (see section 4) suggest that the process is not conservative at such scales, with $H > 0$. Then, the results of direct MA at these small scales remain questionable. Indeed, a strictly positive H parameter would impact the statistics of the process: the latter is expected to be smoothed, leading to attenuated moments when the resolution increases. This could explain the flattening of the empirical moments curve at the largest scales. Figure 5 may be usefully compared with Figure 6 which is the graph of the moments deduced from the absolute gradient of the series, taken at 15 s resolution. Obviously, this new definition of Φ impacts the small-scale statistics which obey to multiscaling statistics between 16 min and 15 s time scales, whereas the large-scale statistics remain scaling down to a 32 min time scale. These results enforce the distinction, advocated in section 4, between a small-scale "integrated" regime and a large-scale "nonintegrated" regime. Both of them seem to have multifractal statistics and are separated by a transition at a 32 min time scale. In the range 3 days to 32 min, the $K(q)$ function, represented in Figure 7, may be fitted with UM exponents $\alpha = 0.31$ and $C_1 = 0.59$, which is more or less coherent with the most common values in the literature (see Table 1 for classical results and Table 3 for all the UM parameters estimated in this study). On the contrary, the statistics in the range 16 min to 15 s do not seem universal, since low, average, and high singularities cannot be simultaneously represented within this model. The "best fit" of $K(q)$ (not shown) near the average singularities ($q = 1$) would involve spurious exponents ($\alpha = 1.10$ and $C_1 = 0.17$), which cannot describe other (lower or higher) singularities. Still, such small-scale statistics combine continuous rain events with periods with a lot of zeros, which are qualitatively different and remain therefore dubious. In the following, we apply two procedures to investigate the scaling behavior of rain while washing out the effect of the zeros. At smaller scales, uninterrupted rain events may be analyzed with the help of MA tools. At larger scales, a weighted MA procedure, that overweights nonzero values, is applied on the data.

5.3. Event Analysis

[27] In this paragraph, the analysis of (almost) uninterrupted rain events is presented. This analysis procedure aims to characterize the variability of rain rates in the interior the

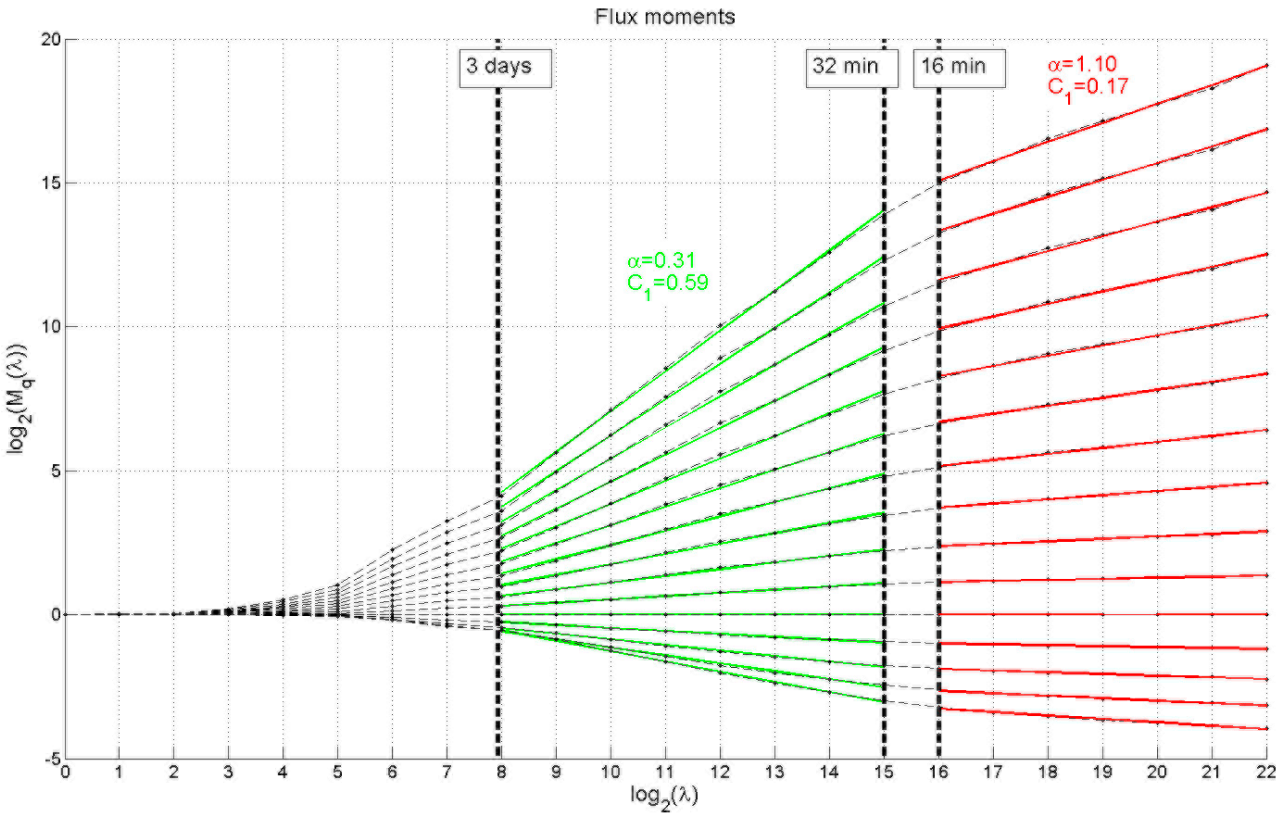

Figure 6. Empirical moments of the absolute gradients of the DBS time series. Scaling regimes are distinguished and fitted with the straight lines, each one for a specific order of moment.

rain events. Rain events were automatically extracted from the full DBS series by taking the greatest consecutive sections that begin with a nonzero rain rate and contain at least 97.5% of nonzero precipitation values. The latter condition enables automatic selection of rainy sequences but implies that the computed moments are conditional statistics in the sense that the presence of high enough singularities is a prerequisite. Among these events, a selection was performed by taking those which have a duration slightly greater than 30 min. Then, all the 52 selected events were truncated in order to have a size of 2^7 points, i.e., a 32 min duration, which is close to the typical size of rain events, as shown by previous spectral analysis. This provides a new data set of rain events of the same size (i.e., a power of two in order to facilitate MA). Then, the procedure described in section 5.1, i.e., inversion of the fractional integration, upscale estimation of the cascade, and estimation of the moments, has been performed on each event. The obtained statistics have then been averaged on all events. It is needed to inverse the fractional integration since, confirming results of Figure 4, a nonconservative behavior (with $H > 0$) appears, as shown on the graph structure function (Figure 8). The moments are represented as a function of the resolution on Figure 9, which shows a good multifractal behavior in the range 32 min to 15 s. The obtained parameters (Figure 10 and Table 3), $\alpha = 1.84$, $C_1 = 0.10$, are notably different from those recalled in Table 1, and from the large-scale parameters estimated in section 5.2, which are obtained by classical analyses that include the zeros. However, such a result is coherent with those obtained by a similar *full-rain* methodology. In the time domain, *de Montera et al.* [2009] estimated $\alpha = 1.7$ and $C_1 = 0.13$ on an event-by-event (small-scale) basis. Moreover, these authors also estimated the nonconservation parameter $H \sim 0.5$ on their rain events,

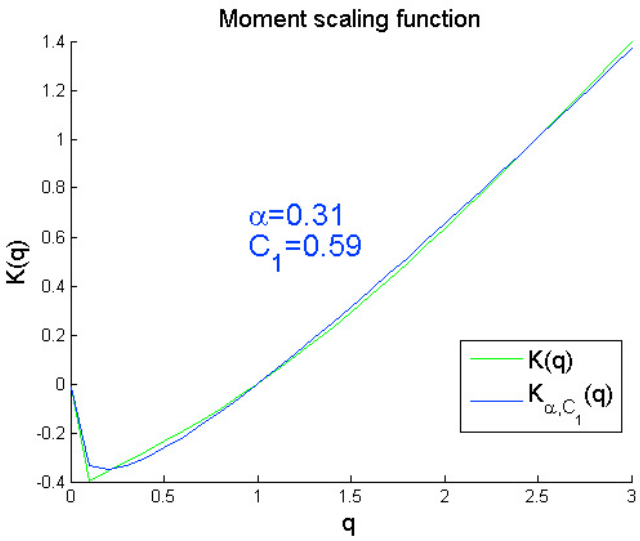

Figure 7. Estimation of empirical moment scaling functions and fit with UM moment scaling functions for the scaling regime 3 days to 32 min.

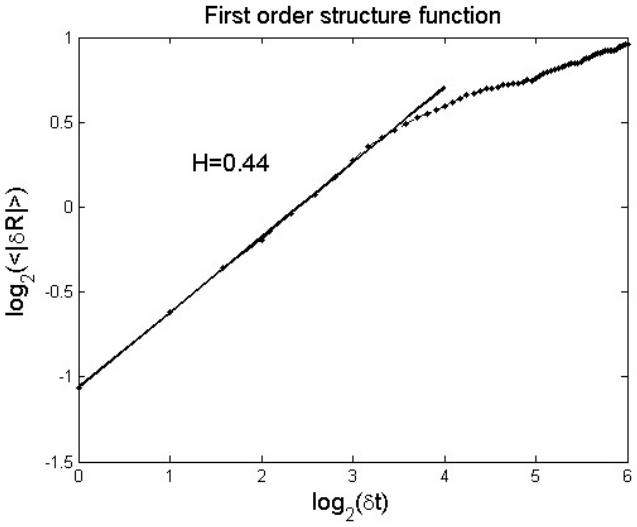

Figure 8. First-order structure function of 52 full-rain events extracted from the DBS series and small-scale fit by linear regression, giving the estimation of H.

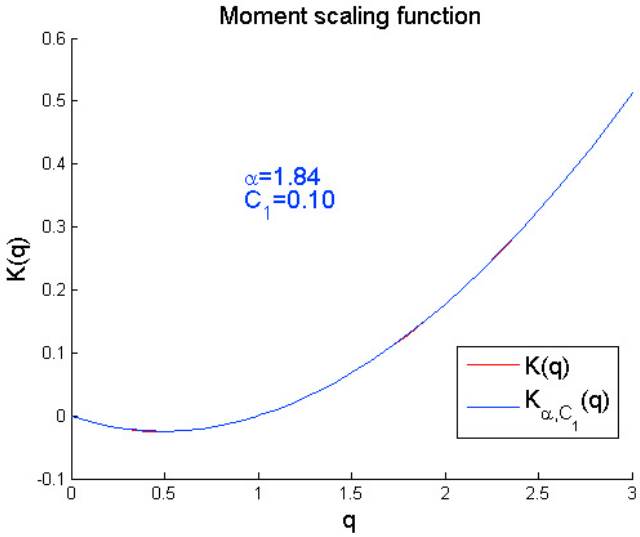

Figure 10. UM fit of empirical moment scaling function of full-rain events, deduced from the fit in Figure 9.

which is consistent with the value reported above. Therefore, a nonconservative multifractal behavior should hold in the interior of rain events.

[28] These remarks are likely to hold in the spatial domain since *Verrier et al.* [2010] estimated $\alpha = 1.8$ and $C_1 = 0.12$ from radar data restricted to full-rain areas (tropical storms), at resolutions between 25 km and 400 m. This should be compared with usual literature parameters in the space domain (see *Lovejoy and Schertzer* [1995] for a review) that provide a smaller α (typically, 1.2–1.4) and a slightly greater C_1 (0.1–0.2). It has been advocated by *de Montera et al.* [2009] and *Verrier et al.* [2010] that most usual literature parameters might suffer from a bias in MA because of the zeros. The more zeros in the series or fields, the greater the bias. For instance, it may be checked that thresholded multifractal fields will have a break and a large-scale biased scaling regime (with $H = 0$) (see *Verrier et al.* [2010] for simulations and the qualitative discussion in section 6.2). A general remark on these full-rain parameters is to notice their similarity in the space and time domains, which is not retrieved in usual literature parameters. This may give some kind of generality to the so-called universal parameters. Yet, the fact that the difference between full-rain and large-scale parameters seems smaller in space does not mean that rain is more space filling in the space domain than in the time domain, but should be rather interpreted as a consequence of preprocessing strategies. Indeed, authors that work in the time domain consider full series with a lot of zeros whereas those who work in the space domain usually preselect maps in order to focus on storms, thus their data contain less zeros.

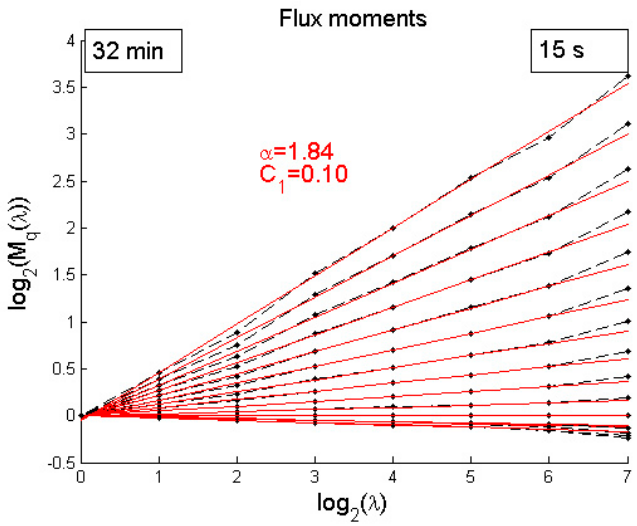

Figure 9. Empirical moments of 52 full-rain events of duration 32 min, extracted from the DBS series, in logarithmic coordinates.

[29] As suggested by recent results [*de Montera et al.*, 2009], the full-rain parameters could be somewhat independent of the place, except perhaps the nonconservativity parameter. On the contrary, rainfall statistics at larger time scales are or seem dependent on local conditions [*Molini et al.*, 2009]. Since large-scale statistics are sensitive to the zeros, there is a need to distinguish between support and microclimatic effects. Another remark on the full-rain parameters is their similarity with those generally used for other atmospheric fields. In a general manner $\alpha \sim 1.8$ and $C_1 \sim 0.1$ define a very current set of multifractal exponents and are likely to model, at least in the space domain, the variability of cloud radiances, cloud liquid water concentration, and perhaps horizontal wind [e.g., *Lovejoy and Schertzer*, 2010].

5.4. Weighted MA of the Data Set

[30] We now investigate the scaling properties of nonzero rain at larger scales. Since, as shown in section 4.2, the data set support has a monoscaling regime between 1.5 day and 32 min time scales, rain values could be seen at these scales as distributed over a fractal support. Because of the latter, the scaling properties of rain are modified (some theoretical

considerations are proposed in section 6.1). In section 5.4, the MA procedure is slightly modified in order to focus on the rain variability only, by removing the effect of the fractal support. We apply a weighted MA (WMA) procedure, originally defined by *Gires* [2009] and *Gires et al.* [2010], in order to compute the coarse scale averages and the empirical moments in a way that overweights the nonzero rain values. The obtained statistics should therefore be representative of rain properties in the interior of its (fractal) support. The procedure is based on the estimation of the statistics of the density with respect to the support and differs from that of section 5.1 by two main changes:

[31] 1. The coarse scale series are computed by averaging neighboring nonzero points (if any), and

[32] 2. The empirical moments are computed using a weighting between the points of the series. When calculating the moments at resolution λ, each interval (or pixel) at this resolution is associated with a weight. The weights are computed by estimating the ratio of the area of the support that intersects the interval by the total area of rain support. Since areas of rain are not well defined in the case of a fractal support, they are approximated by counting the number of rainy subintervals, at the highest available resolution.

[33] Since the fractal scaling of the support is likely to break at 32 min scale (Figure 3), we average the series at 32 min resolution (without any specific weighting) before applying WMA. From the coarse-grained series, WMA provides the moments on the graph represented in Figure 11. A wide scaling regime is observed from 1 week to 32 min time scales. The fit lines intersect at about $\log_2(\lambda) = 4$, i.e., a 1.5 month time scale. This outer scale of the multifractal cascade is comparable to the value of 42 days estimated by *Lovejoy and Schertzer* [2010] from rain gauge data and could be interpreted as the typical lifetime of synoptic structures. The multifractal parameters are estimated at $\alpha = 1.22$ and $C_1 = 0.16$ (Figure 12). Figure 11 leads to think that, when excluding the zeros, rainfall should be multifractal from 32 min (average event duration) to 1 week (which is not so far from synoptic-scale weather structures) time scales, with corrected parameters, different from those estimated in section 5.2 for similar scales. Moreover, the comparison of the (small-scale) event analysis of previous section 5.4 and of WMA reveals a rather limited change in multifractal parameters: in both cases, C_1 is moderate and $\alpha > 1$ is the indicator of processes with unbounded singularities (on the above side).

6. Rain Over a Support: Consequences on Multifractal Analysis and Simulation Procedures

6.1. Rain Over a Support: Which Interpretation?

[34] Section 6.1 aims to propose a way to quantify the biases that occur in MA because of the zeros. Rain data sets often have the property that the nonzero values are distributed over a fractal support, at least in some scaling range. When performing direct MA, as defined in section 5.1, on a rain series with a support dimension $d_f < 1$, some biases may appear. Multifractal fields over a fractal support may exhibit a biased empirical scaling regime when the empirical moments are estimated without taking care of the zeros. The presence of zeros in the series is responsible for inadequate (and unphysical) averagings between zero and nonzero values. Therefore, classical analysis tools will provide a biased estimation, denoted $\hat{K}(q)$, of the moment scaling function $K(q)$. To quantify this, let us first recall the notion of trace moments (for simplicity, we restrict the theoretical developments of section 6.1 to the case $H = 0$).

[35] At resolution λ, the series may be decomposed in λ intervals $]t_1, t_2[\ldots]\ t_\lambda, t_{\lambda+1}[$. At each of these intervals, a total accumulation $X_\lambda(i) = \int_{]t_i, t_{i+1}[} \Phi_\Lambda(t)dt$ may be defined (the maximal resolution is Λ). Classically, the average trace moments [*Schertzer and Lovejoy*, 1987; *Schertzer et al.*, 2002] may be defined:

$$\left\langle Tr\left[\Phi_\lambda^q\right]\right\rangle = \left\langle \sum_{i=1}^{\lambda} X_\lambda(i)^q \right\rangle. \tag{7}$$

[36] For a one-dimensional process, these moments are scaling:

$$\left\langle Tr\left[\Phi_\lambda^q\right]\right\rangle \propto \lambda^{M_1(q)} \tag{8}$$

where:

$$M_1(q) = K(q) - (q-1). \tag{9}$$

[37] In the same way, we have for d-dimensional processes:

$$M_d(q) = K(q) - d(q-1). \tag{10}$$

[38] Following *Schmitt et al.* [1998], it may be noticed that the empirical trace moments involve sums and accumulations only. Therefore, contrary to classical moments, which are sensitive to inadequate averagings between rain values and rain zeros, the moment trace scaling function remains invariant whatever the dimension involved in MA. By inadequately assuming that the process is one dimensional, instead of d_f dimensional, a biased moment scaling function $\hat{K}(q)$ is obtained but the trace moment scaling function is correctly estimated. Hence, we may equal the two expressions:

$$M_{d_f}(q) = K(q) - d_f(q-1) = \hat{K}(q) - d(q-1) \tag{11}$$

which provides the expression of the (biased) empirical moment scaling function:

$$\hat{K}(q) = K(q) + c_f(q-1) \tag{12}$$

where c_f is the fractal codimension of the rain support. It may be noted that the condition of conservativity $\hat{K}(1) = 0$ is accurately followed. However, the fractal support has been taken into account since $\lim_{q\to 0+} \hat{K}(q) = -c_f$. Note that equation (12) quantifies the multiscaling properties of a UM field multiplied by an independent β-model monofractal cascade.

[39] From equation (12), an approximation of the usual biased parameters may be proposed. Indeed, suppose that the universal parameters are estimated by fitting the empirical moment scaling function with the universal two-parameter form for moderate orders. The fit is strongly conditioned by the behavior of the process not too far from

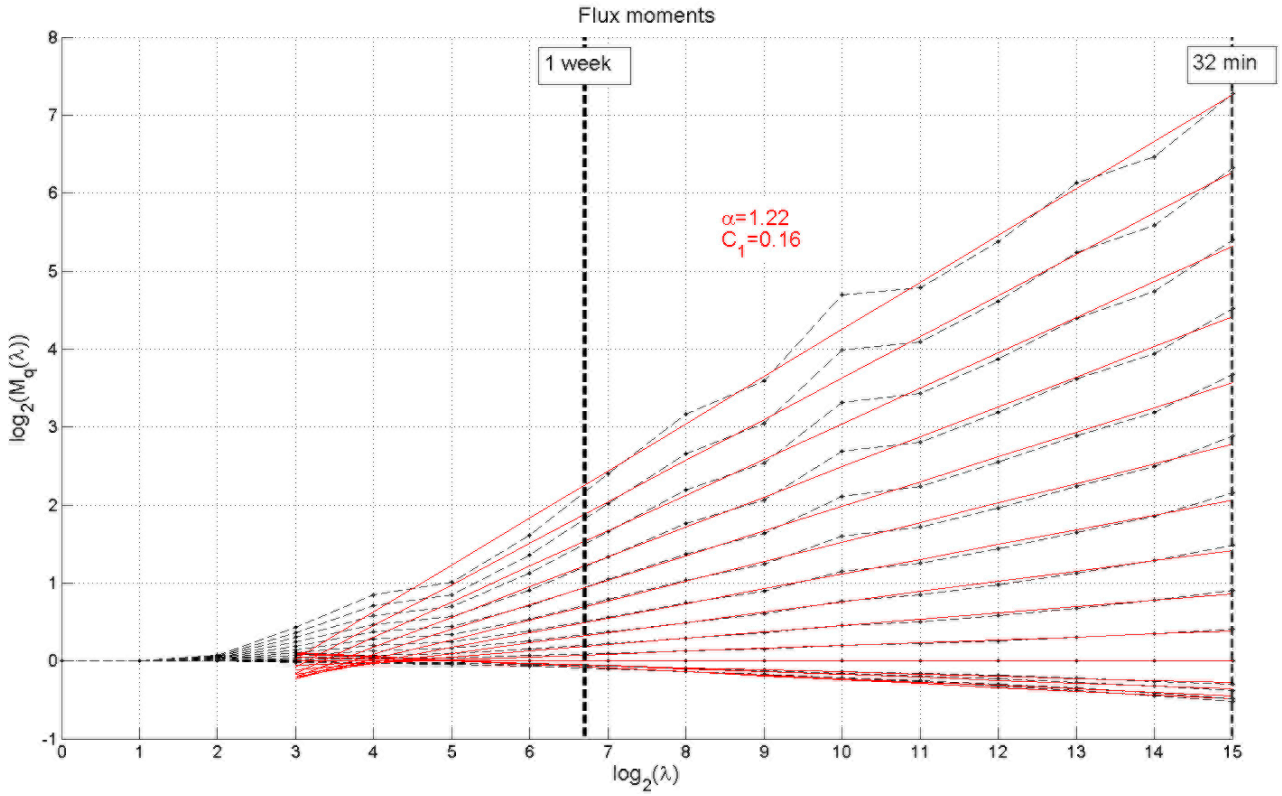

Figure 11. Weighted empirical moments of the DBS time series, as a function of the resolution, in log-log coordinates. Both the resolution degradation process and the weighting procedure are adapted in order to overweight the nonzero rain values.

the mean of the process ($q = 1$). Let us now consider the optimal estimation of the parameters α and C_1, near $q = 1$. When $K(q)$ has a universal form, the parameters may be estimated by considering the derivatives in $q = 1$: $K'(1) = C_1$ and $K''(1) = C_1\alpha$. However, the optimal fit, near the mean of the process, of $\hat{K}(q)$, which does not have the classical form, will provide biased parameters that should follow, with trivial notations:

$$\begin{cases} \hat{K}'(1) = \hat{C}_1 \\ \hat{K}''(1) = \hat{C}_1\hat{\alpha} \end{cases}. \tag{13}$$

[40] From (12) and (13), the values of biased parameters may be expressed as:

$$\hat{C}_1 = C_1 + c_f \tag{14}$$

$$\hat{\alpha} = \frac{\alpha C_1}{C_1 + c_f}. \tag{15}$$

[41] This could explain why MA of rain fields that contain a lot of zeros provides a high value of C_1 and a rather small value of α, compared to full-rain parameters and to parameters that describe other atmospheric processes. In the same way, the spectrum of conservative cascades should be flatter in this pseudoscaling regime:

$$\hat{\beta} = 1 - \hat{K}(2) = \beta - c_f \tag{16}$$

[42] Let us now consider the small-scale and full-rain parameters obtained in section 5.3, i.e., $\alpha = 1.8$, $C_1 = 0.1$. If we assume that these parameters in fact hold at larger scales (where the process becomes nearly conservative, $H \sim 0$), but are distributed at these scales over a fractal support which would bias direct MA, we could try to test the

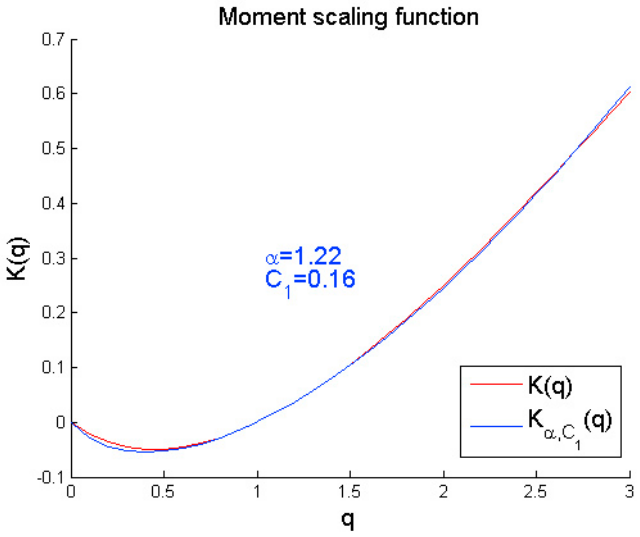

Figure 12. Best UM fit of the moment scaling function of the weighted statistics shown in Figure 11.

above formulas. This is equivalent to wonder which biased UM parameters would be expectable in the range of scales where the data set support has codimension 0.45, i.e., 1.5 days to 30 min. By applying the above formulas, we find $\hat{C}_1 = 0.55$ and $\hat{\alpha} \approx 0.3$, which is very consistent with the large-scale parameters estimated from Figure 6 in the range 3 days to 32 min. In addition, the spectral slope $\hat{\beta} \approx 1.1$ is very close to that estimated from Figure 2 in the range 3 hr to 32 min. The break observed on the power spectrum at 3 h would in fact be independent of the multifractality of the series and only result from a (progressive) transition from nonstationarity ($H \neq 0$) to stationarity ($H = 0$), coherently with the first-order structure function presented in Figure 4.

[43] The model of rain over a support seems therefore pertinent to quantify some biases because of the zero rain rate effect on multifractal statistics, and to explain part (most?) of the differences between parameters of the literature (Table 1) and those reported in Table 3. An apparent multifractal transition between scaling regimes such as those shown in this study could in fact hide some kind of dimensional transition. However, the applicability of the previous formulas should be nuanced since they are based a limited range of order of moments and hence of classes of variability. Moreover, realistic rain supports are coupled with the position of rain peaks which should not be distributed independently of the support borders, which is not adequately represented by the model described this section.

[44] Even though some properties of multifractal processes over a support may be demonstrated, the issue of the simulation of such processes is important for applications. In the section 6.2, some strategies of simulation are reviewed and their main characteristics are discussed.

6.2. How to Simulate Both Rain Variability and Support?

[45] Whereas simple and efficient algorithms for simulating UM or FIF fields are available [*Wilson et al.*, 1991; *Pecknold et al.*, 1993], they are not designed for simulating fields with many zeros. To take the latter into account, we need a procedure that forces the pixels or time intervals that are outside the rain support to zero. Two main solutions have been considered in the literature: (1) multiplying the multifractal field by an independent monofractal support, and, (2) applying a threshold to the synthetic UM or FIF field.

[46] Solution 1 may admit some variants in the way of generating the fractal support. The most classical one [*Over and Gupta*, 1996] is to consider a β-model cascade, which could possibly be adapted to continuity in scale. This model is coherent with the cascade phenomenology and has the advantage that the support dimension can be easily and precisely set to a given value. However, some authors questioned the ability of the a β-model to reproduce adequately the probability distributions of wet and dry sequences durations [*Schmitt et al.*, 1998] and proposed to use alternative solutions such as scaling renewal processes [*Bernardara et al.*, 2007], which are not considered in the following paragraphs.

[47] The basic alternative between solutions 1 and 2 can be commented by comparing their properties. The independent fractal support approach suffers from a lack of correlation between heavy rain structures and support shapes. This approach may be not easily extendable to nonconservative multifractal FIFs. Moreover, a purely monofractal support would have a zero area, which is problematic, unless building a monofractal cascade up to a maximal (finite) resolution. Opposite, solution 2 could appear more appealing since there is a strong coupling between rainfall variability and rainfall support. Since a threshold in rain processes could be given some physical or instrumental justification, this model could seem more physically based. However, such a model could involve subtle effects in the multiscale behavior of the processes, which have been considered in detail by the means of numerical simulations in previous papers [*de Montera et al.*, 2009; *Verrier et al.*, 2010]. These simulations demonstrated that thresholded UM or FIF has biased scaling properties and can exhibit breaks in the scaling. To see how such effects can arise, suppose for instance a conservative UM field and apply a low threshold. Then, a minimal singularity γ_T will be imposed, resulting (after Legendre tranformation) in a linear $K(q)$ function for low q values ($q < q_T$). However, if the threshold is high enough so that $\gamma_T > C_1$ (or equivalently $q_T > 1$), the normalization of the field will be affected and a break will appear in the scaling. In this case, thresholding a multifractal field produces a break in the scaling with a large-scale pseudoscaling regime [*Verrier et al.*, 2010]. The large-scale (pseudo) scaling regime is in fact associated with a fractal support.

[48] As shown in section 5.2, there is strong evidence of a transition separating two multifractal regimes in the DBS data, and the results in sections 5.3, 5.4 and 6.1 have shown that more or less the same underlying multifractal parameters could hold in both regimes, while appearing different because of support effects. It is therefore tempting to interpret this behavior as a consequence of the (unavoidable) instrumental threshold in the data. Because of this threshold, different empirical scaling regimes would appear while possibly hiding a unique underlying multifractal scaling. However, even in this view, the distinction between true zeros and instrumental ones remains rather an open issue. Moreover, we should not forget that the support model has also its own interest, especially because of its mathematical convenience (e.g., applicability of the equations in section 6.1). In fact, the choice of the appropriate model for rainfall simulation might be dependent on the domain of application and of the purposes of the simulation. An alternative possibility would be to combine some of these models. In fact, Figure 3 shows that the rain support is fractal from a few days to half an hour time scale and that at smaller scales, the fractality does not hold because of the lack of rain zeros in rain events. This would suggest to model separately large-scale zeros from small-scale zeros. Hence, a product of a UM or FIF and of a β-model may be sufficient to simulate rain for resolutions greater than half an hour, but simulating finer resolution series would need additional multifractal multiplicative increments with a low threshold.

7. Conclusion

[49] Even though the scaling properties of rain have been investigated in the time domain for a long time, a number of studies were based on data sets with a coarse resolution, typically daily, and did not explore (subdaily and) subhourly scales. This is a drawback since the structure and the internal variability of rain events is missed. In this study, we used a

disdrometer time series of higher resolution (15 s) to show that rainfall processes exhibit remarkable features at subdaily scales. In particular, rain variability presents multifractal properties in separate 3 day to 32 min and 16 min to 15 s scaling regimes. Since the numerous zeros present in the rainfall series were suspected to bias multifractal analysis results and universal multifractal parameters estimates, we proposed to modify analysis procedures in order to estimate more reliable parameters. First, multifractal analysis has been applied to about 50 uninterrupted rain events of duration ~30 min, extracted from the data set. This leads to corrected universal parameters, namely, $\alpha = 1.8$, $C_1 = 0.1$. Then, a weighted multifractal analysis procedure has been applied to the full-rain time series and highlighted the sensitivity of large-scale parameters to the zeros. In order to model and quantify the bias due to the zeros, a model of multifractals distributed over a fractal support was designed, and formulas for the biased universal multifractal parameters were derived, depending on the "true" ones and the codimension of the support. Since the data set support was shown to be scaling in the same large-scale (i.e., from a few days to half an hour) regime as above, these formulas were applicable to our case study. The large-scale biased parameters were retrieved satisfactorily. Therefore, an important correction to usual parameters reported in the literature should be appropriate (from the biased parameters, $\alpha \sim 0.5$, $C_1 \sim 0.5$, to corrected ones, $\alpha \sim 1.8$, $C_1 \sim 0.1$). One challenge remaining for applications involving the simulation of realistic rainfall series would be to define a simulation procedure that will take into account both rain variability and rain support scaling properties, while conserving the correct scaling regimes. The key difficulty may reside in the characterization and interpretation of the rain zeros: how to separate rain and absence of rain, on both physical and instrumental approaches? which is the part of instrumental limitations? The adaptation of existing multiplicative models to a realistic modeling of both rain values and zero rain rates remains an outstanding challenge.

[50] **Acknowledgments.** We are grateful to S. Lovejoy, D. Schertzer, I. Tchiguirinskaia, and A. Gires for fruitful discussions. We also thank the two referees for their helpful comments and suggestions.

References

Bernardara, P., C. de Michele, and R. Rosso (2007), A simple model of rain in time: An alternating renewal process of wet and dry states with a fractional (non-Gaussian) rain intensity, *Atmos. Res.*, *84*, 291–301, doi:10.1016/j.atmosres.2006.09.001.

Corrsin, S. (1951), On the spectrum of isotropic temperature fluctuations in an isotropic turbulence, *J. Appl. Phys.*, *22*, 469–473, doi:10.1063/1.1699986.

Deidda, R. (2000), Rainfall downscaling in a space-time multifractal framework, *Water Resour. Res.*, *36*(7), 1779–1794, doi:10.1029/2000WR900038.

Delahaye, J.-Y., L. Barthès, P. Golé, J. Lavergnat, and J. P. Vinson (2006), A dual-beam spectropluviometer concept, *J. Hydrol.*, *328*, 110–120, doi:10.1016/j.jhydrol.2005.11.048.

de Lima, M. I. P., and J. L. M. P. de Lima (2009), Investigating the multifractality of point precipitation in the Madeira archipelago, *Nonlinear Processes Geophys.*, *16*, 299–311, doi:10.5194/npg-16-299-2009.

de Lima, M. I. P., and J. Grasman (1999), Multifractal analysis of 15-min and daily rainfall from a semi-arid region in Portugal, *J. Hydrol.*, *220*, 1–11, doi:10.1016/S0022-1694(99)00053-0.

de Montera, L., L. Barthès, C. Mallet, and P. Golé (2009), The effect of rain–no rain intermittency on the estimation of the universal multifractals model parameters, *J. Hydrometeorol.*, *10*, 493–506, doi:10.1175/2008JHM1040.1.

de Montera, L., S. Verrier, C. Mallet, and L. Barthès (2010), A passive scalar-like model for rain applicable up to storm scale, *Atmos. Res.*, *98*, 140–147, doi:10.1016/j.atmosres.2010.06.012.

Dubrulle, B. (1994), Intermittency in fully developed turbulence: Log-Poisson statistics and generalized scale covariance, *Phys. Rev. Lett.*, *73*, 959–962, doi:10.1103/PhysRevLett.73.959.

Falkovich, G., A. Fouxon, and M. G. Stepanov (2002), Acceleration of rain initiation by cloud turbulence, *Nature*, *419*, 151–154, doi:10.1038/nature00983.

Fraedrich, K., and C. Larnder (1993), Scaling regimes of composite rainfall time series, *Tellus, Ser. A*, *45*, 289–298, doi:10.1034/j.1600-0870.1993.t01-3-00004.x.

Gires, A. (2009), Intercomparaison multi-échelle des précipitations du modèle Méso-NH avec des données radar, M.S. thesis, Ecole Natl. des Ponts et Chaussées, Marne-la-Vallée, France.

Gires, A., D. Schertzer, I. Tchiguirinskaia, and S. Lovejoy (2010), Multifractal downscaling of precipitation in climate scenarios and a mesoscale model, paper presented at Final Conference of the COST Action C22, Eur. Coop. in Sci. and Technol., Paris.

Gupta, V. K., and E. C. Waymire (1997), Reply, *J. Appl. Meteorol.*, *36*, 1304, doi:10.1175/1520-0450(1997)036<1304:R>2.0.CO;2.

Harris, D., M. Menabde, A. Seed, and G. Austin (1996), Multifractal characterization of rain fields with a strong orographic influence, *J. Geophys. Res.*, *101*(D21), 26,405–26,414, doi:10.1029/96JD01656.

Hubert, P., J. P. Carbonnel, and A. Chaouche (1989), Segmentation des séries hydrométéorologiques: Application à des séries de précipitations et de débits de l'Afrique de l'Ouest, *J. Hydrol.*, *110*, 349–367, doi:10.1016/0022-1694(89)90197-2.

Hubert, P., Y. Tessier, S. Lovejoy, D. Schertzer, F. Schmitt, P. Ladoy, J. P. Carbonnel, S. Violette, and I. Desurosne (1993), Multifractals and extreme rainfall events, *Geophys. Res. Lett.*, *20*(10), 931–934, doi:10.1029/93GL01245.

Hubert, P., I. Tchiguirinskaia, D. Schertzer, H. Bendjoudi, and S. Lovejoy (2007), Predetermination of floods, in *Extreme Hydrological Events: New Concepts for Security*, *NATO Sci. Ser., IV*, edited by O. F. Vasiliev et al., pp. 185–198, vol. 78, Springer, Berlin.

Kolmogorov, A. N. (1962), A refinement of previous hypotheses concerning the local structure of turbulence in a viscous incompressible fluid at high Reynolds number, *J. Fluid Mech.*, *13*, 82–85, doi:10.1017/SLa0022112062000518.

Ladoy, P., S. Lovejoy, and D. Schertzer (1991), Extreme fluctuations and intermittency in climatological temperatures and precipitation, in *Scaling, Fractals and Non-linear Variability in Geophysics*, edited by D. Schertzer and S. Lovejoy, pp. 241–250, Kluwer Acad., Dordrecht, Netherlands.

Ladoy, P., F. Schmitt, D. Schertzer, and S. Lovejoy (1993), Variabilité temporelle multifractale des observations pluviométriques à Nimes, *C. R. Acad. Sci., Ser. II*, *317*, 775–782.

Lavallée, D., S. Lovejoy, D. Schertzer, and P. Ladoy (1993), Nonlinear variability and landscape topography: Analysis and simulation, in *Fractals in Geography*, edited by L. DeCola and N. Lam, pp. 158–192, Prentice Hall, Englewood Cliffs, N. J.

Lavergnat, J., and P. Golé (1998), A stochastic raindrop time distribution model, *J. Appl. Meteorol.*, *37*, 805–818, doi:10.1175/1520-0450(1998)037<0805:ASRTDM>2.0.CO;2.

Lilley, M., S. Lovejoy, N. Desaulniers-Soucy, and D. Schertzer (2006), Multifractal large number of drops limit in rain, *J. Hydrol.*, *328*, 20–37, doi:10.1016/j.jhydrol.2005.11.063.

Lovejoy, S., and D. Schertzer (1995), Multifractals and rain, in *New Uncertainty Concepts in Hydrology and Water Resources*, edited by Z. W. Kundzewicz, pp. 62–103, Cambridge Univ. Press, Cambridge, U. K.

Lovejoy, S., and D. Schertzer (2007), Scale, scaling and multifractals in geophysics: Twenty years on, in *Nonlinear Dynamics in Geosciences*, edited by A. A. Tsonis and J. Elsner, pp. 311–337, Springer, Berlin.

Lovejoy, S., and D. Schertzer (2008), Turbulence, raindrops, and the $l^{1/2}$ number density law, *New J. Phys.*, *10*, 075017, doi:10.1088/1367-2630/10/7/075017.

Lovejoy, S., and D. Schertzer (2010), Towards a new synthesis for atmospheric dynamics: Space-time cascades, *Atmos. Res.*, *96*, 1–52, doi:1016/j.atmosres.2010.01.004.

Lovejoy, S., D. Schertzer, and V. C. Allaire (2008), The remarkable wide range spatial scaling of TRMM precipitation, *Atmos. Res.*, *90*, 10–32, doi:10.1016/j.atmosres.2008.02.016.

Lovejoy, S., J. Pinel, and D. Schertzer (2011), The global space-time cascade structure of precipitation: Satellites, gridded gauges and reanalyses, *Adv. Water Resour.*, in press.

Mandelbrot, B. B. (1974), Intermittent turbulence in self-similar cascades: Divergence of high moments and dimension of the carrier, *J. Fluid Mech.*, *62*, 331–358, doi:10.1017/S0022112074000711.

Marsan, D., D. Schertzer, and S. Lovejoy (1996), Causal space-time multifractal processes: Predictability and forecasting of rain fields, *J. Geophys. Res.*, *101*(D21), 26,333–26,346, doi:10.1029/96JD01840.

Molini, A., G. G. Katul, A. Porporato (2009), Revisiting rainfall clustering and intermittency across different climatic regimes, *Water Resour. Res.*, *45*, W11403, doi:10.1029/2008WR007352.

Obukhov, A. M. (1949), The structure of the temperature field in a turbulent flow, *Izv. Akad. Nauk SSSR, Ser. Fiz.*, *13*, 58–69.

Obukhov, A. M. (1962), Some specific features of atmospheric turbulence, *J. Fluid Mech.*, *13*, 77–81, doi:10.1017/S0022112062000506.

Olsson, J. (1995), Limits and characteristics of the multifractal behaviour of a high-resolution rainfall time series, *Nonlinear Processes Geophys.*, *2*, 23–29, doi:10.5194/npg-2-23-1995.

Olsson, J., J. Niemczynowicz, and R. Berndtsson (1993), Fractal analysis of high-resolution rainfall time series, *J. Geophys. Res.*, *98*(D12), 23,265–23,274, doi:10.1029/93JD02658.

Over, T. M., and V. K. Gupta (1996), A space-time theory of mesoscale rainfall using random cascades, *J. Geophys. Res.*, *101*(D21), 26,319–26,331, doi:10.1029/96JD02033.

Parisi, G., and U. Frisch (1985), A multifractal model of intermittency, in *Turbulence and Predictability in Geophysical Fluid Dynamics and Climate Dynamics*, edited by M. Ghil et al., pp. 84–88, North-Holland, Amsterdam.

Pathirana, A., S. Herath, and T. Yamada (2003), Estimating rainfall distributions at high temporal resolutions using a multifractal model, *Hydrol. Earth Syst. Sci.*, *7*, 668–679, doi:10.5194/hess-7-668-2003.

Pecknold, S., S. Lovejoy, D. Schertzer, C. Hooge, and J. F. Malouin (1993), The simulation of universal multifractals, in *Cellular Automata: Prospects in Astrophysical Applications*, edited by J. M. Perdang and A. Lejeune, pp. 228–267, World Scientific, Hackensack, N. J.

Schertzer, D., and S. Lovejoy (1987), Physical modeling and analysis of rain and clouds by anisotropic scaling multiplicative processes, *J. Geophys. Res.*, *92*(D8), 9693–9714, doi:10.1029/JD092iD08p09693.

Schertzer, D., and S. Lovejoy (1991), Nonlinear geodynamical variability: Multiple singularities, universality and observables, in *Non-linear Variability in Geophysics: Scaling and Fractals*, edited by D. Schertzer and S. Lovejoy, pp. 41–82, Kluwer Acad., Dordrecht, Netherlands.

Schertzer, D., and S. Lovejoy (1997), Universal multifractals do exist!: Comments on "A statistical analysis of mesoscale rainfall as a random cascade", *J. Appl. Meteorol.*, *36*, 1296–1303, doi:10.1175/1520-0450(1997)036<1296:UMDECO>2.0.CO;2.

Schertzer, D., S. Lovejoy, and P. Hubert (2002), An introduction to stochastic multifractal fields, in *Mathematical Problems in Environmental Science and Engineering*, *Ser. Contemp. Appl. Math.*, vol. 4, edited by A. Ern and L. Weiping, pp. 106–179, Higher Educ. Press, Beijing.

Schmitt, F., S. Vannitsem, and A. Barbosa (1998), Modeling of rainfall time series using two-state renewal processes and multifractals, *J. Geophys. Res.*, *103*(D18), 23,181–23,193, doi:10.1029/98JD02071.

She, Z.-S., and E. Levêque (1994), Universal scaling laws in fully developed turbulence, *Phys. Rev. Lett.*, *72*, 336–339, doi:10.1103/PhysRevLett.72.336.

She, Z.-S., and E. C. Waymire (1995), Quantized energy cascade and log-Poisson statistics in fully developed turbulence, *Phys. Rev. Lett.*, *74*, 262–265, doi:10.1103/PhysRevLett.74.262.

Sun, X., and A. P. Barros (2010), An evaluation of the statistics of rainfall extremes in rain gauge observations and satellite-based and reanalysis products using universal multifractals, *J. Hydrometeorol.*, *11*, 388–404, doi:10.1175/2009JHM1142.1.

Tessier, Y., S. Lovejoy, and D. Schertzer (1993), Universal multifractals: Theory and observations for rain and clouds, *J. Appl. Meteorol.*, *32*, 223–250, doi:10.1175/1520-0450(1993)032<0223:UMTAOF>2.0.CO;2.

Tessier, Y., S. Lovejoy, P. Hubert, D. Schertzer, and S. Pecknold (1996), Multifractal analysis and modeling of rainfall and river flows and scaling, causal transfer functions, *J. Geophys. Res.*, *101*(D21), 26,427–26,440, doi:10.1029/96JD01799.

Verrier, S., L. de Montera, L. Barthès, and C. Mallet (2010), Multifractal analysis of African monsoon rain fields, taking into account the zero rain-rate problem, *J. Hydrol.*, *389*, 111–120, doi:10.1016/j.jhydrol.2010.05.035.

Wang, L.-P., and W. W. Grabowski (2009), The role of air turbulence in warm rain initiation, *Atmos. Sci. Lett.*, *10*, 1–8, doi:10.1002/asl.210.

Wilson, J., S. Lovejoy, and D. Schertzer (1991), Physically based cloud modelling by scaling multiplicative cascade processes, in *Scaling, Fractals and Non-linear Variability in Geophysics*, edited by D. Schertzer and S. Lovejoy, pp. 185–208, Kluwer Acad., Dordrecht, Netherlands.

Xue, Y., L.-P. Wang, and W. W. Grabowski (2008), Growth of cloud droplets by turbulent collision-coalescence, *J. Atmos. Sci.*, *65*, 331–356, doi:10.1175/2007JAS2406.1.

Yaglom, A. M. (1966), The influence of the fluctuation in energy dissipation on the shape of turbulent characteristics in the inertial interval, *Sov. Phys. Dokl., Engl. Transl.*, *2*, 26–30.

L. Barthès, C. Mallet, and S. Verrier, LATMOS, CNRS/INSU, Université de Versailles Saint-Quentin-en-Yvelines, 11 Blvd. d'Alembert, F-78280 Guyancourt, France. (verrier@latmos.ipsl.fr)